High-resolution long-reach distributed Brillouin sensing based on combined time-domain and correlation-domain analysis

David Elooz,[1] Yair Antman,[1] Nadav Levanon,[2] and Avi Zadok[1,*]

[1]*Faculty of Engineering, Bar-Ilan University, Ramat-Gan 52900, Israel*
[2]*School of Electrical Engineering, Faculty of Engineering, Tel-Aviv University, Tel-Aviv 69978, Israel*
[*]*Avinoam.Zadok@biu.ac.il*

Abstract: A new scheme for distributed Brillouin sensing of strain and temperature in optical fibers is proposed, analyzed and demonstrated experimentally. The technique combines between time-domain and correlation-domain analysis. Both Brillouin pump and signal waves are repeatedly co-modulated by a relatively short, high-rate phase sequence, which introduces Brillouin interactions in a large number of discrete correlation peaks. In addition, the pump wave is also modulated by a single amplitude pulse, which leads to a temporal separation between the generation of different peaks. The Brillouin amplification of the signal wave at individual peak locations is resolved in the time domain. The technique provides the high spatial resolution and long range of unambiguous measurement offered by correlation-domain Brillouin analysis, together with reduced acquisition time through the simultaneous interrogation of a large number of resolution points. In addition, perfect Golomb codes are used in the phase modulation of the two waves instead of random sequences, in order to reduce noise due to residual, off-peak Brillouin interactions. The principle of the method is supported by extensive numerical simulations. Using the proposed scheme, the Brillouin gain spectrum is mapped experimentally along a 400 m-long fiber under test with a spatial resolution of 2 cm, or 20,000 resolution points, with only 127 scans per choice of frequency offset between pump and signal. Compared with corresponding phase-coded, Brillouin correlation domain analysis schemes with equal range and resolution, the acquisition time is reduced by a factor of over 150. A 5 cm-long hot spot, located towards the output end of the pump wave, is properly identified in the measurements. The method represents a significant advance towards practical high-resolution and long range Brillouin sensing systems.

OCIS codes: (290.5900) Scattering, stimulated Brillouin; (060.2370) Fiber optics sensors; (190.2055) Dynamic gratings; (190.4370) Nonlinear optics, fibers.

References and links

1. R. W. Boyd, *Nonlinear Optics*, 3rd ed. (Academic, 2008).
2. A. Zadok, A. Eyal, and M. Tur, "Stimulated Brillouin scattering slow light in optical fibers [Invited]," Appl. Opt. **50**(25), E38–E49 (2011).
3. T. Kurashima, T. Horiguchi, and M. Tateda, "Distributed-temperature sensing using stimulated Brillouin scattering in optical silica fibers," Opt. Lett. **15**(18), 1038–1040 (1990).
4. T. Horiguchi, T. Kurashima, and M. Tateda, "A technique to measure distributed strain in optical fibers," IEEE Photonics Technol. Lett. **2**(5), 352–354 (1990).
5. M. Niklès, L. Thévenaz, and P. A. Robert, "Simple distributed fiber sensor based on Brillouin gain spectrum analysis," Opt. Lett. **21**(10), 758–760 (1996).
6. X. Bao and L. A. Chen, "Recent progress in Brillouin scattering based fiber sensors," Sensors (Basel) **11**(4), 4152–4187 (2011).

#202197 - $15.00 USD Received 28 Nov 2013; revised 10 Feb 2014; accepted 14 Feb 2014; published 12 Mar 2014

7. S. Martin-Lopez, M. Alcon-Camas, F. Rodriguez, P. Corredera, J. D. Ania-Castañon, L. Thévenaz, and M. Gonzalez-Herraez, "Brillouin optical time-domain analysis assisted by second-order Raman amplification," Opt. Express **18**(18), 18769–18778 (2010).
8. M. A. Soto, G. Bolognini, and F. Di Pasquale, "Long-range simplex-coded BOTDA sensor over 120 km distance employing optical preamplification," Opt. Lett. **36**(2), 232–234 (2011).
9. M. A. Soto, G. Bolognini, and F. Di Pasquale, "Optimization of long-range BOTDA sensors with high resolution using first-order bi-directional Raman amplification," Opt. Express **19**(5), 4444–4457 (2011).
10. Y. Dong, L. Chen, and X. Bao, "Time-division multiplexing-based BOTDA over 100 km sensing length," Opt. Lett. **36**(2), 277–279 (2011).
11. Y. Peled, A. Motil, L. Yaron, and M. Tur, "Slope-assisted fast distributed sensing in optical fibers with arbitrary Brillouin profile," Opt. Express **19**(21), 19845–19854 (2011).
12. Y. Peled, A. Motil, and M. Tur, "Fast Brillouin optical time domain analysis for dynamic sensing," Opt. Express **20**(8), 8584–8591 (2012).
13. Y. Peled, A. Motil, I. Kressel, and M. Tur, "Monitoring the propagation of mechanical waves using an optical fiber distributed and dynamic strain sensor based on BOTDA," Opt. Express **21**(9), 10697–10705 (2013).
14. A. Fellay, L. Thevenaz, M. Facchini, M. Nikles, and P. Robert, "Distributed sensing using stimulated Brillouin scattering: towards ultimate resolution," in *12th International Conference on Optical Fiber Sensors*, Vol. 16 of 1997 OSA Technical Digest Series (Optical Society of America, 1997), paper OWD3.
15. J. C. Beugnot, M. Tur, S. F. Mafang, and L. Thévenaz, "Distributed Brillouin sensing with sub-meter spatial resolution: modeling and processing," Opt. Express **19**(8), 7381–7397 (2011).
16. V. Lecoeuche, D. J. Webb, C. N. Pannell, and D. A. Jackson, "Transient response in high-resolution Brillouin-based distributed sensing using probe pulses shorter than the acoustic relaxation time," Opt. Lett. **25**(3), 156–158 (2000).
17. F. Wang, X. Bao, L. Chen, Y. Li, J. Snoddy, and X. Zhang, "Using pulse with a dark base to achieve high spatial and frequency resolution for the distributed Brillouin sensor," Opt. Lett. **33**(22), 2707–2709 (2008).
18. A. W. Brown, B. G. Colpitts, and K. Brown, "Distributed sensor based on dark-pulse Brillouin scattering," IEEE Photonics Technol. Lett. **17**(7), 1501–1503 (2005).
19. L. Thévenaz and S. F. Mafang, "Distributed fiber sensing using Brillouin echoes," Proc. SPIE **7004**, 70043N (2008).
20. S. Foaleng Mafang, M. Tur, J. C. Beugnot, and L. Thevenaz, "High spatial and spectral resolution long-range sensing using Brillouin echoes," J. Lightwave Technol. **28**(20), 2993–3003 (2010).
21. W. Li, X. Bao, Y. Li, and L. Chen, "Differential pulse-width pair BOTDA for high spatial resolution sensing," Opt. Express **16**(26), 21616–21625 (2008).
22. T. Sperber, A. Eyal, M. Tur, and L. Thévenaz, "High spatial resolution distributed sensing in optical fibers by Brillouin gain-profile tracing," Opt. Express **18**(8), 8671–8679 (2010).
23. Y. Dong, H. Zhang, L. Chen, and X. Bao, "2 cm spatial-resolution and 2 km range Brillouin optical fiber sensor using a transient differential pulse pair," Appl. Opt. **51**(9), 1229–1235 (2012).
24. Y. Antman, N. Levanon, and A. Zadok, "Low-noise delays from dynamic Brillouin gratings based on perfect Golomb coding of pump waves," Opt. Lett. **37**(24), 5259–5261 (2012).
25. K. Hotate and T. Hasegawa, "Measurement of Brillouin gain spectrum distribution along an optical fiber using a correlation-based technique-proposal, experiment and simulation," IEICE Trans. Electron. **E83-C**(3), 405–412 (2000).
26. K. Y. Song, Z. He, and K. Hotate, "Distributed strain measurement with millimeter-order spatial resolution based on Brillouin optical correlation domain analysis," Opt. Lett. **31**(17), 2526–2528 (2006).
27. W. Zou, Z. He, and K. Hotate, "Range elongation of distributed discrimination of strain and temperature in Brillouin optical correlation-domain analysis based on dual frequency modulations," IEEE Sens. J. **14**(1), 244–248 (2014).
28. J. H. Jeong, K. Lee, K. Y. Song, J. M. Jeong, and S. B. Lee, "Differential measurement scheme for Brillouin Optical Correlation Domain Analysis," Opt. Express **20**(24), 27094–27101 (2012).
29. A. Zadok, Y. Antman, N. Primerov, A. Denisov, J. Sancho, and L. Thevenaz, "Random-access distributed fiber sensing," Laser Photonics Rev. **6**(5), L1–L5 (2012).
30. Y. Antman, N. Primerov, J. Sancho, L. Thevenaz, and A. Zadok, "Localized and stationary dynamic gratings via stimulated Brillouin scattering with phase modulated pumps," Opt. Express **20**(7), 7807–7821 (2012).
31. Y. Antman, L. Yaron, T. Langer, M. Tur, N. Levanon, and A. Zadok, "Experimental demonstration of localized Brillouin gratings with low off-peak reflectivity established by perfect Golomb codes," Opt. Lett. **38**(22), 4701–4704 (2013).
32. A. Denisov, M. A. Soto, and L. Thévenaz, "Time gated phase-correlation distributed Brillouin fiber sensor," Proc. SPIE **8794**, 879431 (2013).
33. A. Zadok, E. Zilka, A. Eyal, L. Thévenaz, and M. Tur, "Vector analysis of stimulated Brillouin scattering amplification in standard single-mode fibers," Opt. Express **16**(26), 21692–21707 (2008).

1. Introduction

Stimulated Brillouin Scattering (SBS) is a non-linear effect which can couple between two optical waves along standard optical fibers [1]. In SBS, a relatively intense pump wave

#202197 - $15.00 USD Received 28 Nov 2013; revised 10 Feb 2014; accepted 14 Feb 2014; published 12 Mar 2014

interacts with a counter-propagating, typically weaker signal wave, which is detuned in frequency [1]. The combination of the two waves generates a slowly-traveling intensity wave whose frequency equals the difference between the frequencies of the pump and signal waves, and its wavenumber is the sum of their wavenumbers. Through electrostriction, the intensity wave introduces traveling density variations, namely an acoustic wave, which in turn leads to a traveling grating of refractive index variations due to the photo-elastic effect. The traveling grating can couple optical power between the counter-propagating pump and signal waves. Effective coupling, however, requires that the difference between the two optical frequencies should closely match a particular, fiber-dependent value known as the *Brillouin frequency shift* ν_B ~11 GHz (for standard single mode fibers at ~1550 nm wavelength). The power of a signal wave whose optical frequency is ν_B below that of the pump is amplified by SBS. The amplification bandwidth achieved with continuous-wave (CW) pumping is rather narrow: on the order of 30 MHz, as dictated by the relatively long lifetime of acoustic phonons [1, 2].

The value of ν_B varies with both temperature and mechanical strain [3]. Hence, a mapping of the local Brillouin gain spectrum along standard fibers is being used in distributed sensing of both quantities for 25 years [4–6]. The most widely employed configuration for such measurements is known as Brillouin optical time domain analysis (B-OTDA), in which pump pulses are used to amplify CW signals and the output signal power is monitored as a function of time [4]. Experiments are repeated for a range of frequency offsets $\nu \sim \nu_B$ between pump and signal. The measurement range of B-OTDAs could reach 100 km [7–10], and they are capable, at least in principle, of mapping the SBS gain for a given ν along the entire fiber with just a single scan. The acquisition times of B-OTDA setups were recently reduced to the order of ms for 100 m-long fibers [11–13]. However, the duration of pulses in the fundamental B-OTDA scheme is restricted to the acoustic lifetime τ ~5 ns or longer, which corresponds to a spatial resolution limitation on the order of 1 m [14]. Numerous schemes had been proposed in recent years for resolution enhancement in B-OTDA [6,15], such as the pre-excitation of the acoustic wave [16,17], dark [18] and π-phase [19,20] pump pulses, repeated measurements with pump pulses of different widths [21], differentiation of the signal power [22] and many more. B-OTDA setups had reached spatial resolutions of 2 cm over 2 km of fiber [23].

The strength of the acoustic field at a given fiber location is closely related to the inner product between the complex envelopes of the pump and signal waves, weighted over a window that is 2τ long [24]. The spatial pattern of the acoustic field strength is therefore directly associated with the temporal cross-correlation between the envelopes of the counter-propagating waves [24]. Starting in the late 90's, Hotate and associates had proposed to modulate the two waves so that their envelopes are correlated at discrete points of interest only, referred to as *correlation peaks* [25]. The technique came to be known as Brillouin optical correlation domain analysis, or B-OCDA, and it effectively confines the SBS interaction to the correlation peaks, where it is stationary. Initial demonstrations relied on the joint frequency modulation of the pump and signal, which are nominally detuned by a certain ν, by a common sine wave [25]. While providing mm-scale resolution [26], initial B-OCDA was restricted to an unambiguous measurement range of a few hundreds of resolution points only, limited by the separation between neighboring periodic peaks. The measurement range was since extended using more elaborate frequency modulation profiles [27,28].

In our previous work, in collaboration with the Thevenaz group at EPFL [29], we extended the B-OCDA principle to the joint phase modulation of the pump and signal waves by a common, high-rate pseudo-random bit sequence (PRBS) [29,30]. The modulation effectively confines the SBS interaction to correlation peaks whose spatial extent corresponds to that of a single coding symbol. Using 12 Gbit/s phase modulation, a spatial resolution of 9 mm had been achieved [29]. At the same time, the separation between neighboring peaks is governed by the length of the code, which can be arbitrarily long. Unambiguous

#202197 - $15.00 USD Received 28 Nov 2013; revised 10 Feb 2014; accepted 14 Feb 2014; published 12 Mar 2014

measurements at the above resolution were carried out over sections of a 200 m long fiber, or the equivalent of more than 20,000 potential resolution points.

PRBS phase modulation effectively decouples between range and resolution in B-OCDA. The method does suffer, however, from two primary drawbacks which are common to many B-OCDA implementations. First, although the off-peak acoustic field vanishes on average, its instantaneous value is nevertheless nonzero and fluctuating [24]. Residual off-peak reflectivity accumulates over the entire length of the fiber and severely degrades the signal-to-noise ratio (SNR) of the measurements. A large number of averages over repeated measurements are necessary to overcome this so-called 'coding noise' [24,31]. Second, the Brillouin gain spectrum must be mapped one spatial point at a time, scanning the entire length of the fiber in due course. The undertaking of tens of thousands of individual scans for every ν, using laboratory equipment, often proves impractical. For example, in [29] we were able to scan an entire 40 m-long fiber with 1 cm resolution, but could not do the same for the entire 200 m-long fiber, due to excessive acquisition times.

An important step towards SNR improvement was made by Denisov *et al.* [32], who overlaid ns-scale amplitude pulse modulation on top of the PRBS phase coding of the pump wave. Using synchronized, time-gated measurements of the output signal, they were able to reduce the coding noise substantially and preform 1 cm-resolution measurements over a 3 km-long fiber. Their work can be regarded as a merger between B-OTDA and B-OCDA principles. Nevertheless, the issue of serial point-by-point acquisition still remained, and the complete mapping of the Brillouin gain spectrum over the entire set of 300,000 potential resolution points could not be performed.

In this work, we propose and demonstrate a combined B-OTDA / B-OCDA technique, which addresses both the measurement SNR and acquisition time. As in [32], an amplitude-pulsed pump and a CW signal are both phase modulated by a joint sequence, following the B-OCDA principle. However, two significant advances are introduced: First, a short, perfect Golomb code is used in the phase modulation of the pump and signal waves instead of a long PRBS. The special correlation properties of this sequence help reduce the coding noise considerably [24,31]. Second, due to the short length of the code, a large number of correlation peaks are generated during the propagation of the pump wave pulse. With careful choice of the pump pulse duration with respect to the Golomb code period and the Brillouin lifetime τ, the SBS amplification which takes place at the different peaks can be temporally resolved in measurements of the output signal power, much like in a B-OTDA. Using this method, the number of scans per choice of ν that is necessary for mapping the Brillouin gain spectrum over the entire fiber equals the length of the Golomb code only, which is 127 bits-long in our case. This number of scans is orders-of-magnitude smaller than that of an equivalent PRBS-coded B-OCDA, and it does not increase with the number of resolution points.

The experimental mapping of the Brillouin gain spectrum over a 400 m-long fiber with 2 cm resolution is reported below. The entire 20,000 resolution points are mapped by only 127 scans per choice of ν, representing a reduction of the acquisition time by a factor of about 150. A 5 cm-long hot spot is properly recognized and localized in the measurements. The technique might provide the breakthrough that is necessary to make high-resolution, long-range Brillouin-sensing more practical.

2. Principle of operation

The B-OTDA principle is known for many years, and has been explained at length in many references [3]. The phase modulation-encoded B-OCDA concept was described in detail in our earlier works [29,30]. The mathematical analyses of both will not be repeated here. We turn instead to the formulation of the SBS interaction between pump and signal waves that are modulated according to the combined technique which is the topic of the current work. We

#202197 - $15.00 USD Received 28 Nov 2013; revised 10 Feb 2014; accepted 14 Feb 2014; published 12 Mar 2014

show later that the spatial-temporal profiles of both B-OTDA and phase-encoded B-OCDA can be obtained as specific cases of the analysis provided below.

Let us denote the optical fields of the pump and signal waves as $E_p(t,z)$ and $E_s(t,z)$ respectively, were z denotes position along a fiber of length L and t represents time. The pump wave enters the fiber at $z=0$ and propagates in the positive z direction, whereas the signal wave propagates from $z=L$ in the negative z direction. We denote the complex envelopes of the pump and signal as $A_p(t,z)$ and $A_s(t,z)$ respectively, and their optical angular frequencies by ω_p and ω_s. The difference between the two frequencies: $\omega_p-\omega_s=\Omega=2\pi\nu$ is on the order of $\Omega_B=2\pi\nu_B$.

In the proposed scheme, the signal envelope at its point of entry into the fiber is modulated by a phase sequence c_n with a symbol duration T that is much shorter than the acoustic lifetime τ:

$$A_s\left(z=L,t\right)=A_{s0}\sum_n c_n \mathrm{rect}\left[\frac{t-nT}{T}\right]\equiv A_s\left(t\right) \tag{1}$$

Here A_{s0} is a constant magnitude, c_n is a prefect Golomb phase code of unity magnitude that is repeated every N symbols, and $\mathrm{rect}(\xi)$ equals 1 for $|\xi|\le 0.5$ and zero elsewhere [24]. The pump wave envelope is also modulated by the same code, as in [24,29–31]. Unlike our earlier works, however, additional amplitude modulation by a single pulse is overlaid on top of the phase sequence:

$$A_p\left(z=0,t\right)=A_{p0}\mathrm{rect}\left(\frac{t}{\theta}\right)\sum_n c_n \mathrm{rect}\left[\frac{t-nT}{T}\right]\equiv A_p\left(t\right) \tag{2}$$

In Eq. (2), A_{p0} is a constant magnitude and θ is the duration of the pump amplitude pulse. The phase sequence symbol duration T and the pulse duration θ are chosen so that $\theta\approx NT>\tau$.

The magnitude of the acoustic field at a given location is given by [30]:

$$Q(t,z)=jg_1\int_0^t \exp\left[-\Gamma_A\left(t-t'\right)\right]A_p\left(t'-\frac{z}{v_g}\right)A_s^*\left(t'-\frac{z}{v_g}-\Delta\left(z\right)\right)dt' \tag{3}$$

Here g_1 is a parameter which depends on the electrostrictive coefficient, the speed of sound and the density of the fiber [1], v_g is the group velocity of light in the fiber, and the position-dependent temporal offset $\Delta(z)$ is defined as $\Delta(z)\equiv(2z-L)/v_g$ [30]. The spatial profile of the acoustic field is therefore closely associated with the cross-correlation between the two modulating envelopes. The exponential weighing bandwidth Γ_A is determined by the choice of the optical frequencies offset ν: $\Gamma_A(\Omega,z)\equiv j\left[\left(\Omega_B^2(z)-\Omega^2-j\Omega\Gamma_B\right)/2\Omega\right]$. It reduces to half the Brillouin linewidth: $\Gamma_A=\frac{1}{2}\Gamma_B=1/(2\tau)$, when $\Omega=\Omega_B$. Note that the Brillouin frequency shift might be position-dependent.

Equation (3) can be integrated numerically, subject to the boundary conditions of Eq. (1) and Eq. (2). Figure 1 shows the magnitude of acoustic field $|Q(z,t)|$ over a 6 m-long fiber section, subject to the modulation scheme of pump and signal described above. A uniform ν_B was assumed, and the frequency offset ν was chosen to match that value. A perfect Golomb code ($N=127$, $T=200\,\mathrm{ps}$, see Appendix) was used in the phase modulation of both pump and signal, and a 26 ns-long amplitude pulse was superimposed on the phase-modulated

#202197 - $15.00 USD Received 28 Nov 2013; revised 10 Feb 2014; accepted 14 Feb 2014; published 12 Mar 2014

pump wave. As expected in phase-encoded B-OCDA [29,30], the acoustic field is confined to a discrete set of spatially-periodic correlation peaks, whose width $\Delta z = \frac{1}{2} v_g T$ equals 2 cm in this case. The separation between neighboring peaks is $N \cdot \Delta z$. Unlike the previous scheme, however, the temporal duration of each correlation peak is restricted to the order of θ, and the peaks do not overlap in the time domain. The power of the output signal, at any given instance, would be affected by SBS amplification in a single correlation peak or by none at all.

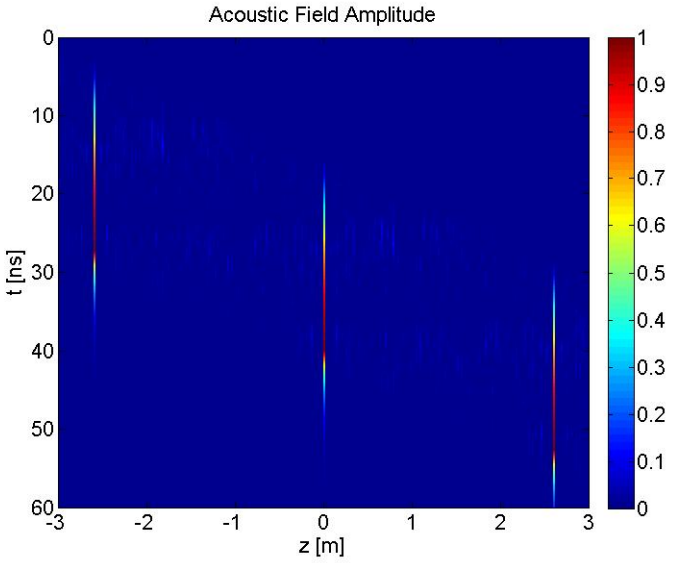

Fig. 1. Simulated magnitude of the acoustic wave density fluctuations (in normalized units), as a function of position and time along a 6 m-long fiber section. Both pump and signal waves are co-modulated by a perfect Golomb phase code that is 127 bits long (see Appendix), with symbol duration of 200 ps. The pump wave was further modulated by a single amplitude pulse of 26 ns duration (see Eq. (1) and Eq. (2)). The acoustic field, and hence the SBS interaction between pump and signal, is confined to discrete and periodic narrow correlation peaks. The peaks are built up sequentially one after another with no temporal overlap.

Figure 2 shows the simulated output signal power as a function of time $\left|A_s\left(z=0,t\right)\right|^2$. The trace consists of a series of amplification peaks, each of which can be unambiguously related to the SBS interaction at a specific correlation peak of known location. A single trace therefore provides information on $L/\left(N \cdot \Delta z\right) >> 1$ fiber positions. The locations of the correlation peaks can be offset in Δz increments with proper retiming of the phase modulation of the pump and signal [29,30]. The correlation peaks would return to their initial locations every N steps, hence N scans would be sufficient for the mapping of the Brillouin gain over the entire fiber, for each choice of ν. This number of scans does not depend on the fiber length, and is orders-of-magnitude smaller than the number of resolution points $L/\Delta z$. The combined technique retains the high resolution and long range of unambiguous measurement that is provided by phase-encoded B-OCDA, with an acquisition time that is potentially much reduced. In addition, use of perfect Golomb codes instead of PRBS phase modulation reduces the coding noise substantially [24,31], and may help decrease the necessary number of averages.

#202197 - $15.00 USD Received 28 Nov 2013; revised 10 Feb 2014; accepted 14 Feb 2014; published 12 Mar 2014

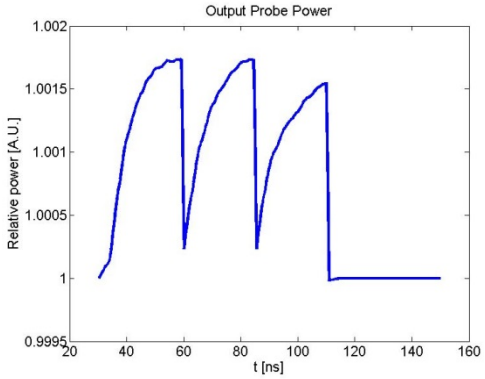

Fig. 2. Simulated output signal power as a function of time. The trace consists of a series of amplification peaks, each of which can be unambiguously related to the SBS interaction at a specific correlation peak (see Fig. 1).

For comparison, Fig. 3 shows the calculated $|Q(z,t)|$ for the phase-coded B-OCDA scenario ($\theta \to \infty$,panel (a)), and for the B-OTDA case ($c_n = 1$ for all n , panel (b)). The SBS interaction in B-OTDA at any given instance spreads over a comparatively large spatial extent, restricting resolution. Use of short codes in B-OCDA, on the other hand, leads to ambiguous measurements of the output signal power due to the simultaneous generation of multiple peaks.

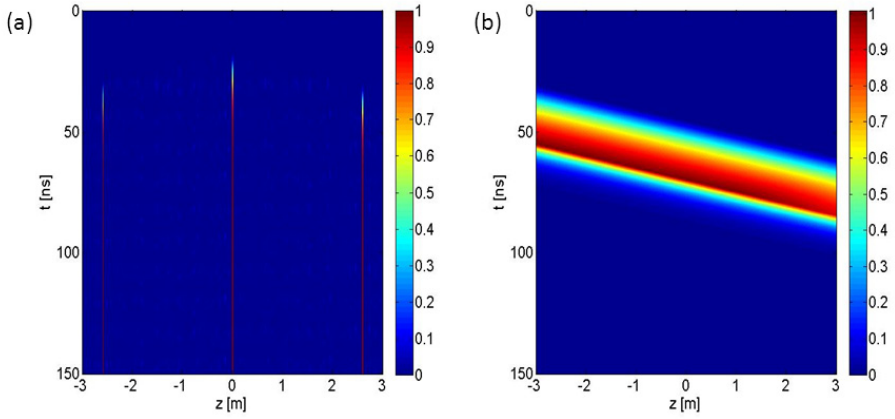

Fig. 3. Simulated magnitude of the acoustic wave density fluctuations (in normalized units), as a function of position and time along a 6 m-long fiber section. Panel(a): both pump and signal waves are co-modulated by a perfect Golomb phase code that is 127 bits long, with symbol duration of 200 ps. The simultaneous generation of multiple, periodic correlation peaks would lead to ambiguous measurement of the SBS amplification in monitoring the output signal power. Panel (b): The pump wave was modulated by a single amplitude pulse of 10 ns duration, whereas the signal wave was continuous (B-OTDA). Resolution limitations are illustrated.

3. Experimental setup and results

Figure 4 shows the experimental setup for high-resolution, extended-range Brillouin analysis using the proposed, combined B-OTDA / B-OCDA technique. Both pump and signal waves were drawn from a single laser diode source at 1550 nm wavelength. An electro-optic phase modulator at the laser output was driven by an arbitrary waveform generator (AWG). The

#202197 - $15.00 USD Received 28 Nov 2013; revised 10 Feb 2014; accepted 14 Feb 2014; published 12 Mar 2014

AWG was programmed to repeatedly generate a 127 bits-long perfect Golomb code (see Appendix), with a symbol duration on the order of 200 ps. The output voltage of the generator was adjusted to match $V_\pi \approx 3.7\,\mathrm{V}$ of the modulator.

The phase-modulated light was split into pump and signal branches by a 50/50 fiber coupler. Light in the pump branch was amplitude-modulated by a sine-wave of frequency ν, in suppressed-carrier format. The upper modulation sideband was retained by a narrow-band fiber-Bragg grating (FBG), whereas any residual carrier and the lower sideband were blocked. The pump wave was then modulated again by a second amplitude electro-optic modulator, driven by repeating pulses with a low duty cycle. The pulses duration of 26 ns was chosen to approximately match the period of the Golomb code, and their period of 4 μs exceeded the time-of-flight through the fibers under test. Pulses were then amplified by an erbium-doped fiber amplifier (EDFA) to an average power of 100 mW. A polarization scrambler was used to prevent polarization-related fading of the SBS interaction [33]. Light in the signal branch was delayed in a 4 km-long fiber imbalance [29]. The signal and pump waves were launched into opposite ends of a fiber under test. The signal wave at the output of the fiber under test was detected by a photo-detector of 200 MHz bandwidth, and sampled by a real-time digitizing oscilloscope.

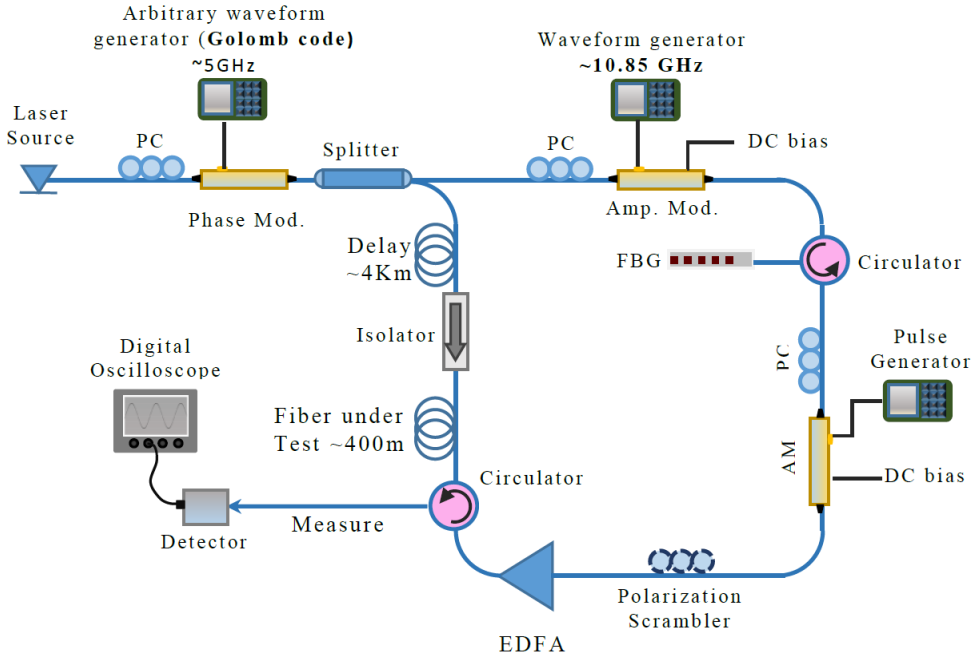

Fig. 4. Experimental setup for combined B-OTDA / B-OCDA distributed sensing.

Arbitrary locations along the fiber under test were addressed as follows [29]: The joint phase modulation introduced multiple correlation peaks along the fiber ring that encompassed the pump branch, the signal branch, and fiber under test (see Fig. 4). The peaks were separated by $N \cdot \Delta z = \frac{1}{2} N v_g T \approx 2.6\,\mathrm{m}$. Hence the position of all peaks, except for the central one, varied with the symbol duration. The 4 km-long path imbalance along the signal branch guaranteed that off-centered correlation peaks were in overlap with the fiber under test. The position of these peaks could be scanned through slight changes to the Golomb code symbol duration: a 23.5 kbit/s variation in the nominal 5 Gbit/s phase modulation rate corresponded to an offset of the correlation peaks by Δz of 2 cm.

#202197 - $15.00 USD Received 28 Nov 2013; revised 10 Feb 2014; accepted 14 Feb 2014; published 12 Mar 2014

Figure 5 shows examples of the output signal as a function of time $\left|A_s\left(z=0,t\right)\right|^2$. The fiber under test consisted of two segments, each about 200 m-long, with ν_B values at room temperature of 10.90 GHz and 10.84 GHz, respectively. A 5 cm-long hot spot was introduced towards the output end of the pump wave. Periodic peaks can be seen in the output probe power, separated by $NT \approx 26\,\text{ns}$ as expected. Each peak corresponds to the SBS amplification of the signal wave at a single correlation peak, as discussed in the previous section. In Fig. 5(a) ν was set to match ν_B of the second fiber at room temperature. A single gain peak which is in overlap with the hot-spot appears weaker (see inset). That specific gain peak is more pronounced than all others when ν was changed to 10.89 GHz, the Brillouin shift in the hot spot (Fig. 5(b), see inset). Each trace was averaged over 64 pump pulses, in order to overcome polarization scrambling variations, coding and thermal noises. Note that the amplification peaks in the first fiber section disappear in Fig. 5(a), due to the mismatch in Brillouin frequency shifts.

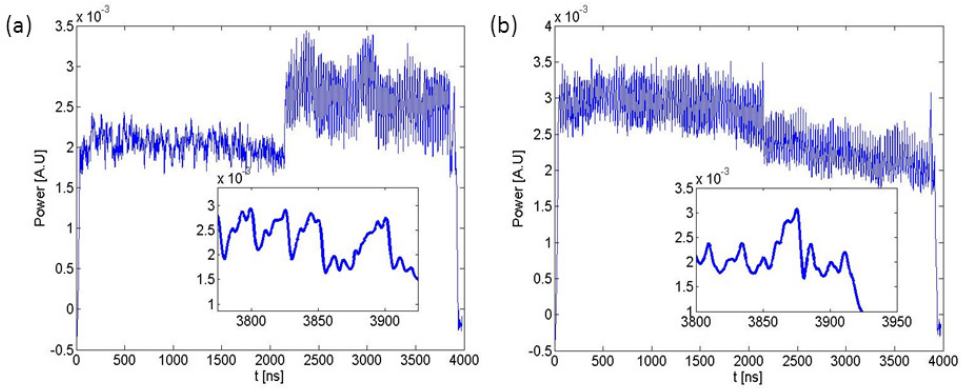

Fig. 5. Measurements of the output signal power as a function or time, following propagation in a 400 m-long fiber under test that was consisted of two sections, each of ~200 m length. The Brillouin frequency shifts of the two segments at room temperature were 10.90 and 10.84 GHz, respectively. Multiple peaks are evident, each corresponding to the SBS amplification in a specific correlation peak of the Golomb code. A 5 cm-long hot spot was located towards the output end of the pump wave. In both panels, one of the correlation peaks is in spatial overlap with the hot spot. The frequency offset between the pump and signal was set to match the Brillouin shift of the second section at room temperature (panel (a), 10.84 GHz), and the Brillouin shift at the temperature of the hot spot (panel (b), 10.89 GHz).

Figure 6 shows the SBS signal gain as a function of ν and z. The experimental procedure effectively reconstructed the Brillouin gain spectra at all 20,000 resolution points using only 127 scans for each choice of ν. The recovered values of $\nu_B\left(z\right)$ are shown in Fig. 7. The hot spot is well recognized (see inset).

#202197 - $15.00 USD Received 28 Nov 2013; revised 10 Feb 2014; accepted 14 Feb 2014; published 12 Mar 2014

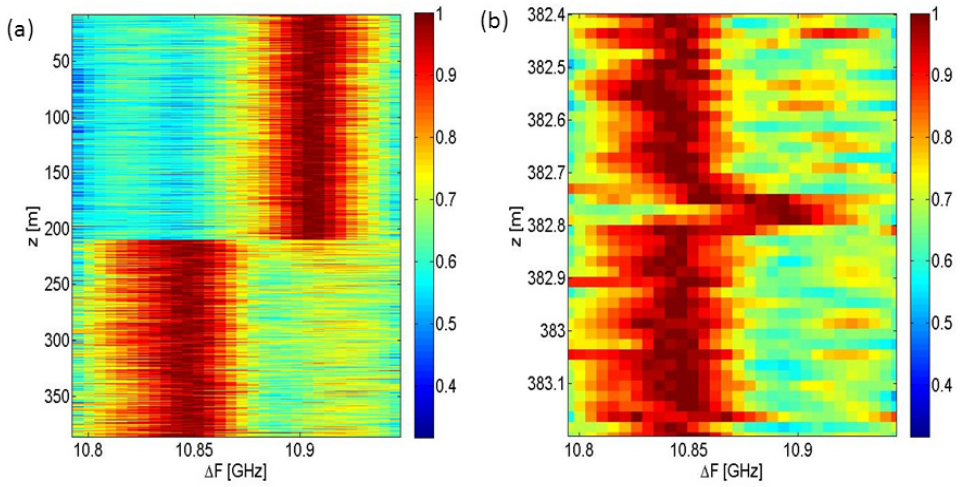

Fig. 6. Measured Brillouin gain map as a function of frequency offset between pump and signal, and position along a 400 m-long fiber under test. The fiber consisted of two sections, each approximately 200 m-long, with Brillouin shifts at room temperature of approximately 10.84 GHz and 10.90 GHz, respectively. A 5 cm-long hot spot was located towards the output end of the pump wave. The map was reconstructed using only 127 scans per frequency offset, according to the combined B-OTDA / B-OCDA method. The complete map is shown on panel (a), and a zoom-in on the hot spot region is shown on panel (b).

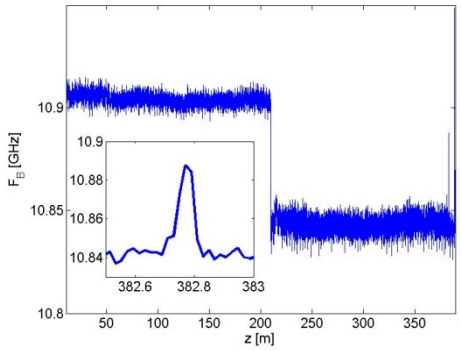

Fig. 7. Brillouin frequency shift as a function of position, as extracted from the experimental Brillouin gain map of Fig. 6 above.

4. Summary

In this work, we have proposed and demonstrated a combined B-OTDA / B-OCDA technique for distributed fiber-optic measurements of strain and temperature. Both SBS pump and signal are repeatedly co-modulated by a short and high-rate phase sequence, whose symbol duration is on the order of hundreds of ps and its period is somewhat longer than the Brillouin lifetime. In addition, the pump wave is also amplitude-modulated by a single pulse, whose duration equals the period of the phase sequence. The method provides the high resolution and long range of unambiguous measurements of phase-coded B-OCDA setups, with two significant improvements: a) Golomb phase codes are used instead of random sequences, and effectively reduce noise due to residual, off-peak Brillouin interactions; and b) The SBS amplification at a large number of correlation peaks is interrogated by the single pump pulse, and resolved in the time domain. The number of scans that is necessary to reconstruct the Brillouin gain for a specific frequency offset ν equals the length of the Golomb code. The

#202197 - $15.00 USD Received 28 Nov 2013; revised 10 Feb 2014; accepted 14 Feb 2014; published 12 Mar 2014

number of scans is smaller than that of a corresponding phase-coded B-OCDA by over two orders of magnitude, and does not increase with the length of fiber under test.

The Brillouin gain spectrum was experimentally acquired over a 400 m-long fiber under test with 2 cm resolution. The entire set of 20,000 resolution points was mapped in only 127 scans per choice of frequency offset ν. A 5 cm-long hot spot, located towards the output end of the pump wave, was properly identified in the measurements. Each trace was averaged over 64 times. The overall acquisition time, for 40 values of ν, was about 1 second. The estimate does not include latencies due to data transfer by laboratory equipment and off-line signal processing, which would be performed in real-time by a realistic, dedicated instrument.

The uncertainty in the estimates of the local Brillouin shift was ± 3 MHz. These rather large variations can be reduced using a larger number of averages. The spatial resolution in the experiments was limited to 2 cm by the rate of waveform generators available to us. The technique is scalable to resolution below 1 cm [29]. Higher resolution measurements would be associated with weaker SBS amplification, and stronger coding noise due to longer Golomb codes. Therefore, the necessary number of averages is expected to increase with resolution.

The technique represents a significant advance towards practical high-resolution, long-range Brillouin analysis. On-going work is dedicated to the reduction of the necessary number of averages, the extension of the measurement range beyond 1 km, and the employment of the technique in the monitoring of structures.

Appendix: Perfect Golomb code

The Golomb code used in the experiments and simulations is 127 bits long. All elements in the code are of unity magnitude. The phases of the following elements equal $\cos^{-1}(-63/64)$: {1 2 4 8 9 11 13 15 16 17 18 19 21 22 25 26 30 31 32 34 35 36 37 38 41 42 44 47 49 50 52 60 61 62 64 68 69 70 71 72 73 74 76 79 81 82 84 87 88 94 98 99 100 103 104 107 113 115 117 120 121 122 124}. The phases of all other elements equal zero.

Acknowledgments

This work was supported in part by the Chief Scientist Office, the Israeli Ministry of Industry, Trade and Labor, through the KAMIN program.

#202197 - $15.00 USD Received 28 Nov 2013; revised 10 Feb 2014; accepted 14 Feb 2014; published 12 Mar 2014